

# Directionality Analysis on Functional Magnetic Resonance Imaging during Motor Task using Granger Causality\*

A R Anwar\*\*, M Muthalib, S Perrey, A Galka, O Granert, S Wolff, G Deuschl, J Raethjen, U Heute  
*Member, IEEE* and M Muthuraman

**Abstract**— Directionality analysis of signals originating from different parts of brain during motor tasks has gained a lot of interest. Since brain activity can be recorded over time, methods of time series analysis can be applied to medical time series as well. Granger Causality is a method to find a causal relationship between time series. Such causality can be referred to as a directional connection and is not necessarily bidirectional. The aim of this study is to differentiate between different motor tasks on the basis of activation maps and also to understand the nature of connections present between different parts of the brain. In this paper, three different motor tasks (finger tapping, simple finger sequencing, and complex finger sequencing) are analyzed. Time series for each task were extracted from functional magnetic resonance imaging (fMRI) data, which have a very good spatial resolution and can look into the sub-cortical regions of the brain. Activation maps based on fMRI images show that, in case of complex finger sequencing, most parts of the brain are active, unlike finger tapping during which only limited regions show activity. Directionality analysis on time series extracted from contralateral motor cortex (CMC), supplementary motor area (SMA), and cerebellum (CER) show bidirectional connections between these parts of the brain. In case of simple finger sequencing and complex finger sequencing, the strongest connections originate from SMA and CMC, while connections originating from CER in either direction are the weakest ones in magnitude during all paradigms.

**Keywords**—fMRI; Granger Causality; Multivariate Autoregressive (MVAR); AIC.

## I. INTRODUCTION

Our study of human brain is based on the idea of considering it as a set of correlated variables in a complex

network. Correlation between these variables helps us mapping simultaneously activated regions of brain both in context of motor tasks and also in absence of such events [1] [2]. Recently, interest has been growing in understanding the underlying dynamic directional relationship between these variables. Such directionality analysis is likely to shed light on the effect of a certain part of the brain on another part and thus can be very helpful in understanding the functional connectivity of human brain [3] [4] [5].

Functional magnetic resonance imaging (fMRI) can measure activity indirectly from all brain regions, using BOLD signal, but suffers from very low temporal resolution, making it prone to missing brain dynamics faster than the sampling rate of fMRI. Functional connectivity of brain can be quantified by analysis of time series from activated regions of interest [6]. The Granger causality (GC) test is one such method which can find functional network connectivity by analysis of time series recorded from different parts of the brain. Calculation of GC is based on multivariate autoregressive (MAR) modeling and the idea behind GC is that causes precede effects [7]. Various directionality analysis methods, based on GC, have recently been applied on medical time series and have given promising results. Such methods include “directed transfer function” (DTF) [8], “partial directed coherence” (PDC) [9], “modified directed transfer function” (dDTF) [10], “generalized partial directed coherence” (gPDC) [11], and “renormalized partial directed coherence” (rPDC) [12]. In order to understand the underlying functional connectivity of brain, we will employ time domain Granger Causality, which has recently been successfully used on fMRI time series [13] [14].

## II. GRANGER CAUSALITY

Conditional GC is based on the principle that an inclusion of past values of time series  $X_1$  improves the predictability of future values of time series  $X_2$ , in comparison to taking into account only the past values of time series  $X_2$ . Such a case implies that time series  $X_1$  Granger causes time series  $X_2$ . Consider three time series  $X_1(t)$ ,  $X_2(t)$  and  $X_3(t)$  given by the following autoregressive model:

\* Research supported by SFB 855 project D2.

\*\*A R Anwar and U Heute are with the Department of Digital Signal Processing and System Theory, University of Kiel, 24143-Kiel, Germany (e-mail: [ara@tf.uni-kiel.de](mailto:ara@tf.uni-kiel.de), [uh@tf.uni-kiel.de](mailto:uh@tf.uni-kiel.de)).

M Muthuraman, O Granert, J Raethjen and G Deuschl are with the Department of Neurology, University of Kiel, 24105-Kiel, Germany (e-mail: [m.muthuraman@neurologie.uni-kiel.de](mailto:m.muthuraman@neurologie.uni-kiel.de), [o.granert@neurologie.uni-kiel.de](mailto:o.granert@neurologie.uni-kiel.de), [j.raethjen@neurologie.uni-kiel.de](mailto:j.raethjen@neurologie.uni-kiel.de), [g.deuschl@neurologie.uni-kiel.de](mailto:g.deuschl@neurologie.uni-kiel.de)).

A Galka is with the Department of Neuropediatrics, University of Kiel, 24105-Kiel, Germany (e-mail: [a.galka@pedneuro.uni-kiel.de](mailto:a.galka@pedneuro.uni-kiel.de)).

S Wolff is with the Department of Neuroradiology, University of Kiel, 24105-Kiel, Germany (e-mail: [s.wolff@neurorad.uni-kiel.de](mailto:s.wolff@neurorad.uni-kiel.de)).

M Muthalib is with the Propulsys Team, University of Montpellier, 34090-Montpellier, France and also with the Faculty of Health, Queensland University of Technology, 4059-Brisbane, Australia (e-mail: [makii.muthalib@univ-montpl.fr](mailto:makii.muthalib@univ-montpl.fr))

S Perrey is with Faculty of Sports Sciences, University of Montpellier, 34090-Montpellier, France (e-mail: [stephane.perrey@univ-montpl.fr](mailto:stephane.perrey@univ-montpl.fr))

$$X_1(t) = \sum_{j=1}^P A_{11j} X_1(t-j) + \sum_{j=1}^P A_{12j} X_2(t-j) + \sum_{j=1}^P A_{13j} X_3(t-j) + \eta_1(t) \quad (1)$$

$$X_2(t) = \sum_{j=1}^P A_{21j} X_1(t-j) + \sum_{j=1}^P A_{22j} X_2(t-j) + \sum_{j=1}^P A_{23j} X_3(t-j) + \eta_2(t) \quad (2)$$

$$X_3(t) = \sum_{j=1}^P A_{31j} X_1(t-j) + \sum_{j=1}^P A_{32j} X_2(t-j) + \sum_{j=1}^P A_{33j} X_3(t-j) + \eta_3(t) \quad (3)$$

Here,  $P$  is the model order ( $P < T$ ),  $T$  is length of time series.  $\eta(t)$  is the prediction error of time series  $X(t)$  and  $A_{xx}$  are the MVAR coefficients.

Assuming that  $X_1(t)$ ,  $X_2(t)$  and  $X_3(t)$  are covariance-stationary, the magnitude of conditional GC from  $X_2(t)$  to  $X_1(t)$  conditioned on  $X_3(t)$  can be given as:

$$F_{2 \rightarrow 1|3} = \ln \frac{\rho_{11}}{\sum_{11}} \quad (4)$$

where  $\rho_{11}$  is subset of noise covariance matrix of restricted model omitting variable 2 and  $\sum_{11}$  is subset of noise covariance matrix of unrestricted model. For further description of this formula, please refer to [15].

Estimation of 'P' is of vital importance while fitting MVAR model to a time series, because choosing a very low order is likely to miss out temporal dynamics of a time series while choosing a higher model order will yield spurious results. In this study, an optimum model order was found using Akaike's Information Criterion (AIC) and conditional Granger causality was applied on modeled and medical time series using the Granger causality connectivity analysis (GCCA) toolbox [15] [16].

No correction for multiple comparisons was performed and conditional GC amplitudes were tested against a significance level calculated using a surrogate-data method. The essential feature of this method is to randomly select blocks with appropriate length from the original time series. These blocks are rejoined to produce re-sampled time series. Due to this random shuffling of blocks, causality in re-sampled time series is lost. Conditional Granger causality, calculated for this re-sampled time series, can be used as a null hypothesis [17].

### III. MODEL DATA

Prior to conditional GC analysis on fMRI time series, it is tested on simulated data. Three time series (Length=2000) of order three were constructed having inbuilt causality given as:

$$X_1(t) = 1.34 * X_1(t-1) - 0.90 * X_1(t-2) + \varepsilon_1(t) \quad (5)$$

$$X_2(t) = 0.50 * X_1(t-2) + \varepsilon_2(t) \quad (6)$$

$$X_3(t) = -0.40 * X_1(t-3) + \varepsilon_3(t) \quad (7)$$

Here,  $\varepsilon(t)$  is white noise. This model is subjected to analysis and directionality was successfully revealed as given below:



Figure 1. Results of directionality analysis on model data.

After testing the method with modeled data, we will now apply it to actual medical time series in the next section.

### IV. EXPERIMENT

Four healthy subjects (two males, two females, mean age = 26) were asked to perform the following three motor tasks for ten minutes with the right hand while fMRI was recorded: Finger tapping (FT), Rigorous tapping of index finger at a frequency of 2-5Hz. Simple finger sequencing(SFS), Tapping sequence of thumb against first, middle, ring and little finger. Complex finger sequencing(CFS), Tapping sequence of thumb against first, ring, middle and little finger. BOLD-sensitive MRI was performed with a 3-Tesla MR scanner (Philips Achieva, Philips, Best, the Netherlands) and a standard 8-channel SENSE head coil. A single-shot T2-weighted, gradient-echo planar-imaging sequence was used for fMRI (TR = 2500 ms, TE = 45 ms, 32 slices,  $64 \times 64$  matrix, slice thickness = 3.5 mm, FOV = 200 mm, flip angle =  $90^\circ$ ). 240 brain volumes were acquired during 10 minutes. Block design was used to find activation maps with a 30-second motor task followed by 30 seconds of rest (10 repetitions).

After recording fMRI, scans were realigned to remove head-movement artifacts. The first image in a session was specified as a reference and all subsequent images were realigned to it. After realignment, images were resliced and normalized. Finally the images were smoothed by convolving them with a full width half-maximum (FWHM) Gaussian kernel of fixed width [ $8 \times 8 \times 8$  mm], in order to suppress noise. Threshold value was fixed to  $p=0.05$  (FWE corrected) with 10 voxels threshold on the cluster extent. Time series were extracted from three regions of the brain, namely contralateral motor cortex (CMC), supplementary motor area (SMA) and cerebellum (CER). For extraction of time series, a sphere of radius 3mm was assumed as a source in the desired part of the brain. Spheres were defined around local Maxima in respective region of brain. Moreover Hemodynamic response function (HRF) of the brain is assumed to be the same all over the brain. No second level analysis was performed and preprocessing of images and time series extraction was done using the SPM8 toolbox (<http://www.fil.ion.ucl.ac.uk/spm>).

### V. RESULTS

Activation maps were overlaid with standard anatomical brain images to locate the exact positions of activity.

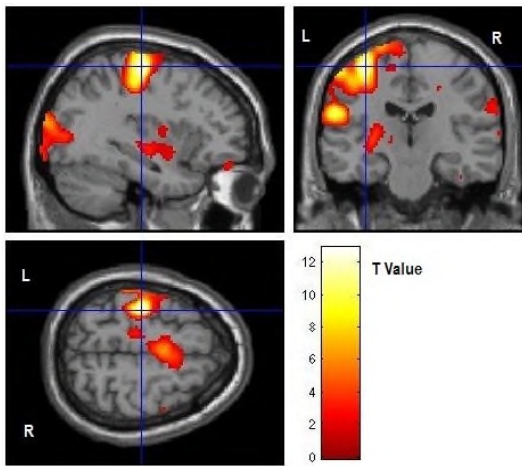


Figure 2. Activation map for finger-tapping activity, with the cross hair showing the contralateral motor cortex as most active region. Example of single subject. Local Maxima (MNI coordinate [-34,-20, 60]).

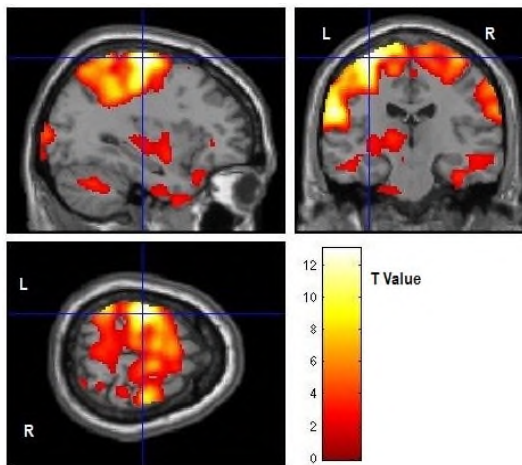


Figure 3. Activation map for simple finger-sequence activity, more brain regions are active as compared to the finger-tapping task. Example of single subject. Local Maxima (MNI coordinate [-32,-20, 68]).

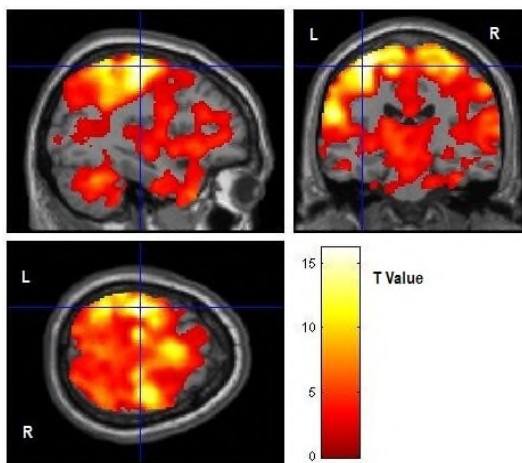


Figure 4. Activation map for complex finger-sequence activity; brain activity can be observed almost all over the brain region. Example of single subject. Local Maxima (MNI coordinate [-36,-22, 62]).

Above activation maps, obtained from single subject, clearly shows that, during complex finger sequencing, more regions of the brain are active than in simple finger-tapping

tasks which have very limited activity in the brain. Moreover, since all subjects were right-handed and activity was performed with the dominant hand, the left side of the brain shows more activity than the right hemisphere. The cross hair shows the approximate location of CMC in all figures (2, 3, and 4).

In order to measure the activation, the number of active voxels was counted, in typical subject, for each activity, as shown in Table I. We can see that CFS has most active voxels while FT has the fewest active voxels. This trend was observed in all subjects except one.

TABLE I  
NUMBER OF ACTIVE VOXELS FOR EACH ACTIVITY

Activity	Number of Activated Voxels
FT	3884
SFS	14360
CFS	46456

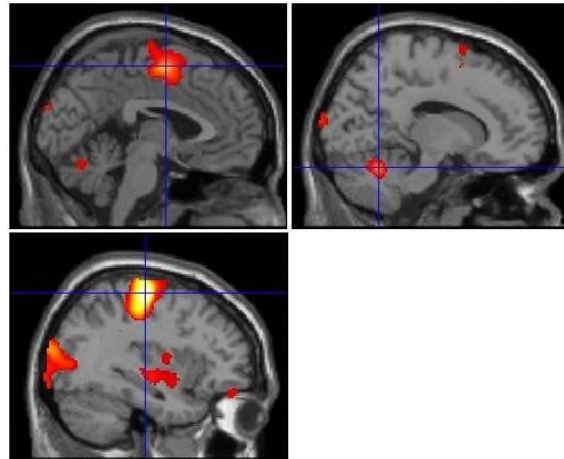


Figure 5. Approximate locations of supplementary motor area (top left), cerebellum (top right) and contralateral motor cortex (bottom left) shown by the cross hair, taken from finger-tapping activity (MNI coordinates [-2,-4, 58], [14,-58,-24], [-34,-20, 60]).

After extracting time series from CMC, SMA, and CER (as shown in Fig 5.), individual time series were subjected to detrending and removing the mean, which is a pre-requisite of MVAR-model fitting. The time series are tested if they are covariance-stationary using the “augmented Dickey Fuller test”, since causality analysis methods cannot be applied to non-stationary time series. An appropriate model order is selected using AIC and conditional granger causality is calculated. The significance level is calculated using surrogate data. Almost all connections were found to be significant, their magnitudes were noted down, and an average was taken over all subjects (see Fig. 6). However, we did not perform any group level studies.

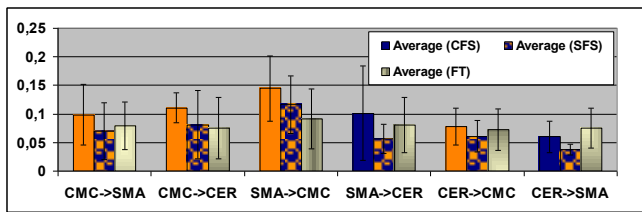


Figure 6. Average connection strength for each motor activity.

From the results, we can see that, especially in case of complex and simple finger sequence, the strongest connection was originating from SMA and CMC, while cerebellum had weakest outgoing connections in all tasks. In order to test the strength of the connections in each case, connections were arranged in order of strength of magnitude.

TABLE II  
STRONGEST CONNECTION IN EACH MOTOR TASK

Activity	Strongest Connection
CFS	SMA -> CMC (75%)
SFS	SMA -> CMC (60%)
FT	CMC -> CER (40%)

Table II. Shows that incase of complex finger sequence, SMA to CMC connection were strongest in 75% of the subjects. In case of simple finger sequence, the strongest connection was again from SMA to CMC in 60% of the subjects, and in case of finger tapping, the strongest connection was from CMC to CER almost 40% of the subjects.

## VI. CONCLUSION

In the presented study, three different motor tasks have been investigated with respect to causality in brain. The results suggest that, incase of complex brain activity, different parts of the brain interact with each other more strongly than during simple finger tapping. In turn, this means that complex activity demands more neural computations from more parts of the brain. This is most likely due to increased emphasis on motor-initiation processes. During simple-sequencing and complex finger-sequencing tasks, the strongest connection observed was from SMA to CMC; however, in case of a finger-tapping task, the strongest connection was observed from CMC to CER. The weakest connections in all tasks are the ones originating from CER to the other two regions of the brain. Both CMC and SMA together act as motor-command signal sources.

## VII. ACKNOWLEDGMENT

Support from the German Research Council (Deutsche Forschungsgemeinschaft, DFG, SFB 855, Project D2) is gratefully acknowledged.

## REFERENCES

- [1] Steven L. Bressler, Anil K. Seth, "Wiener-Granger causality: a well established methodology." *Neuroimage*. 2011 September 15; 58(2): 323–329.
- [2] Zhenyu Zhou; Yun Jiao; Tianyu Tang; Zuhong Lu; Yijun Liu; Yonghong Chen; Mingzhou Ding; , "Detecting Effective Connectivity in Human Brain using Granger Causality," *BioMedical Engineering and Informatics*, 2008. *BMEI 2008. International Conference on* , vol.2, no., pp.394-398, 27-30 May 2008
- [3] Barrett AB , Murphy M , Bruno M-A , Noirhomme Q , Boly M , et al. 2012 "Granger Causality Analysis of Steady-State Electroencephalographic Signals during Propofol-Induced Anaesthesia". *PLoS ONE* 7(1) G. O. Young, "Synthetic structure of industrial plastics (Book style with paper title and editor)," in *Plastics*, 2nd ed. vol. 3, J. Peters, Ed. New York: McGraw-Hill, 1964, pp. 15–64.
- [4] Rainer Goebel, Alard Roebroeck, Dae-Shik Kim, Elia Formisano. "Investigating directed cortical interactions in time-resolved fMRI data using vector autoregressive modeling and Granger causality mapping". *Magn Reson Imaging*. 2003 December; 21(10): 1251–1261.
- [5] Lucy Lee, Lee M Harrison, Andrea Mechelli. "A report of the functional connectivity workshop, Dusseldorf 2002". *Neuroimage*. 2003 June; 19(2 Pt 1): 457–465.
- [6] Martin Havlicek, Jiri Jan, Milan Brazdil, Vince D. Calhoun. "Dynamic Granger causality based on Kalman filter for evaluation of functional network connectivity in fMRI data." *Neuroimage*. 2010 October 15; 53(1): 65–77.
- [7] C. W. J. Granger. *Investigating Causal Relations by Econometric Models and Cross-spectral Methods*. *Econometrica* , Vol. 37, No. 3 (Aug., 1969), pp. 424-438.
- [8] M J Kamiński, K J Blinowska. "A new method of the description of the information flow in the brain structures." *Biol Cybern*. 1991; 65(3): 203–210.
- [9] L A Baccalá, K Sameshima. "Partial directed coherence: a new concept in neural structure determination." *Biol Cybern*. 2001 June; 84(6): 463–474.
- [10] Anna Korzeniewska, Małgorzata Mańczak, Maciej Kamiński, Katarzyna J Blinowska, Stefan Kasicki. "Determination of information flow direction among brain structures by a modified directed transfer function (dDTF) method." *J Neurosci Methods*. 2003 May 30; 125(1-2): 195–207.
- [11] Baccald, L.A.; de Medicina, F.; "Generalized Partial Directed Coherence," *Digital Signal Processing, 2007 15th International Conference on* , vol., no., pp.163-166, 1-4 July 2007.
- [12] Björn Schelter, Jens Timmer, Michael Eichler. "Assessing the strength of directed influences among neural signals using renormalized partial directed coherence." *J Neurosci Methods*. 2009 April 30; 179(1): 121–130.
- [13] Anna Gaglianese, Mauro Costagli, Giulio Bernardi, Emiliano Ricciardi, Pietro Pietrini. "Evidence of a direct influence between the thalamus and hMT + independent of V1 in the human brain as measured by fMRI." *NeuroImage*, Available online 25 January 2012.
- [14] Alkan, Y.; Alvarez, T.L.; Gohel, S.; Taylor, P.A.; Biswal, B.B. , "Functional connectivity in vergence and saccade eye movement tasks assessed using Granger Causality Analysis," *Engineering in Medicine and Biology Society, EMBC, 2011 Annual International Conference of the IEEE* , vol., no., pp.8114-8117, Aug. 30 2011-Sept. 3 2011.
- [15] Anil K. Seth. "A MATLAB toolbox for Granger causal connectivity analysis." *J Neurosci Methods*. 2010 February 15; 186(2): 262–273.
- [16] Akaike, H.; "A new look at the statistical model identification," *Automatic Control, IEEE Transactions on* , vol.19, no.6, pp. 716- 723, Dec 1974.
- [17] M Kamiński, M Ding, W A Truccolo, S L Bressler. "Evaluating causal relations in neural systems: granger causality, directed transfer function and statistical assessment of significance." *Biol Cybern*. 2001 August; 85(2): 145–157.